

Chapter 11: Regional Climate Projections

Coordinating Lead Authors: Jens Hesselbjerg Christensen and Bruce Hewitson

Lead Authors: Aristita Busuioc, Anthony Chen, Xuejie Gao, Isaac Held, Richard Jones, Won-Tae Kwon, René Laprise, Victor Magaña, Linda Mearns, Claudio Menendez, Jouni Räisänen, Annette Rinke, Rupa Kumar Kolli, Abdoulaye Sarr, Penny Whetton

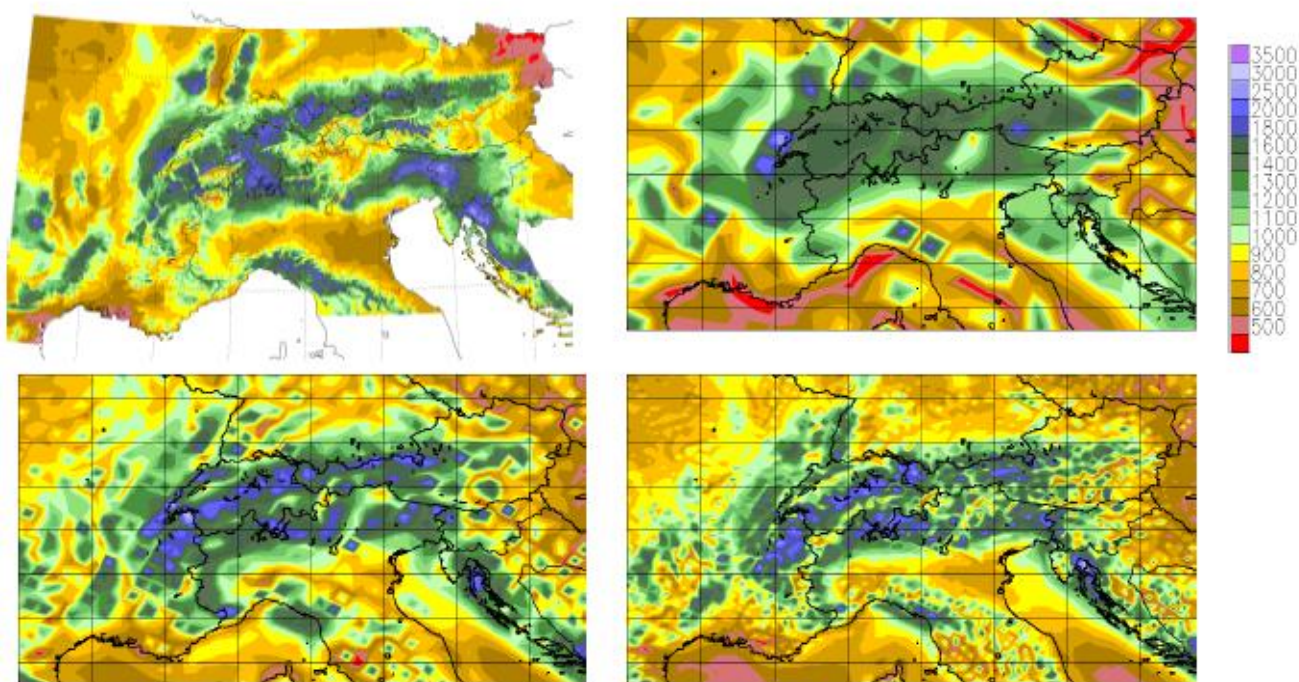
Contributing Authors: Rasmus Benestad, Martin Beniston, David Bromwich, Daniel Caya, Josefino Comiso, Ramón de Elía, Klaus Dethloff, Seita Emori, Johannes Feddema, Ruediger Gerdes, Fidel Gonzales-Rouco, William J. Gutowski, Inger Hansen-Bauer, Colin Jones, Robert Katz, Akio Kitoh, Reto Knutti, Ruby Leung, Jason Lowe, Amanda Lynch, Christoph Matulla, Kathleen McInnes, Anna V. Mescherskaya, Brett Mullan, Mark New, Majid Habibi Nokhandan, Jeremy S. Pal, David Plummer, Markku Rummukainen, Christoph Schär, Samuel Somot, Ramasamy Suppiah, Mark Tadross, Claudia Tebaldi, Warrant Tennant, Martin Widman, Rob Wilby

Review Editors: Congbin Fu, Filippo Giorgi

Date of Draft: 6 March 2006

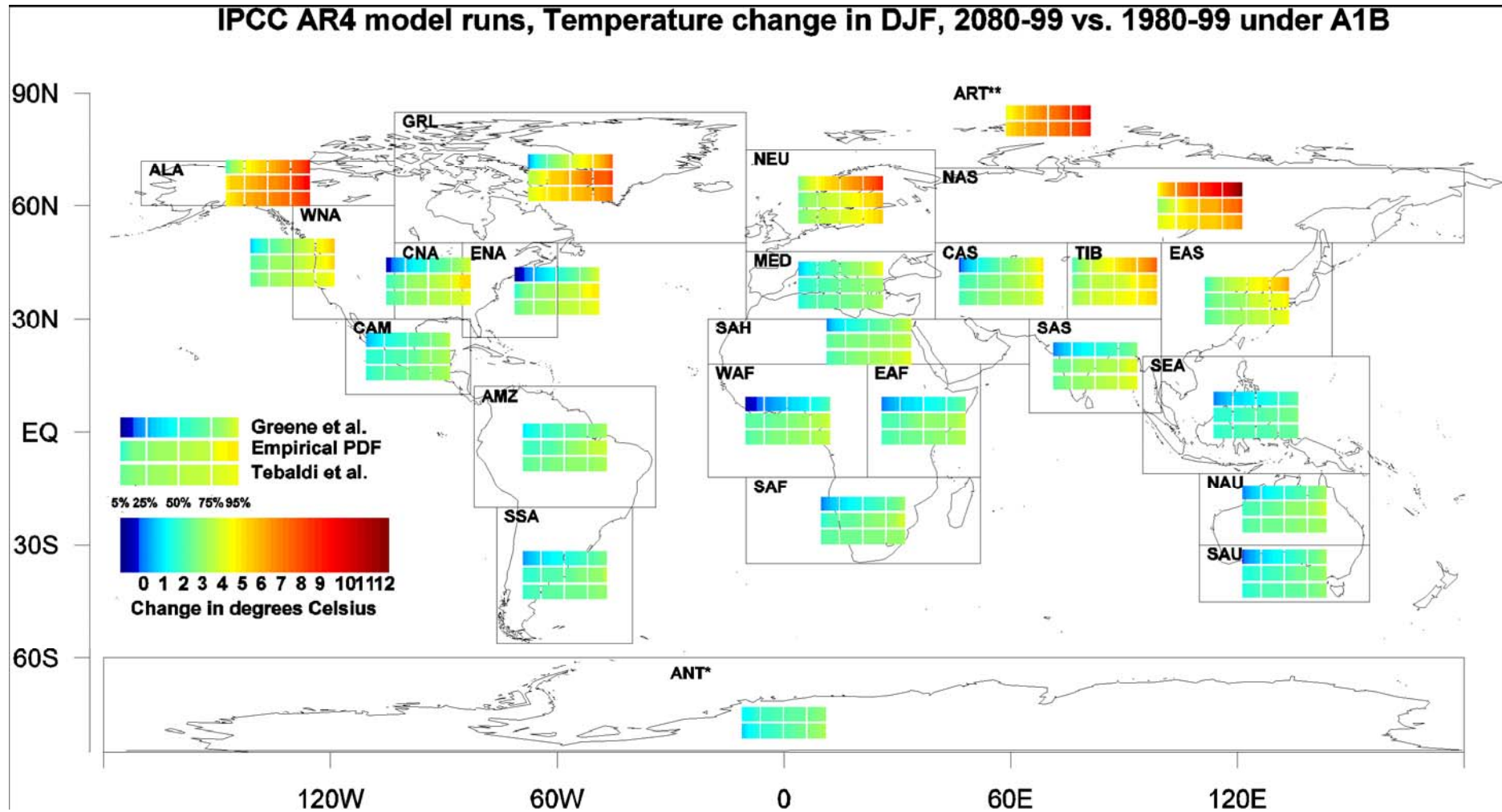
Notes: TSU compiled version

1 **Figures**
 2
 3



4 **Figure 11.1.1.** Annual mean precipitation for the European Alps (in mm). Upper left: Observational analysis
 5 (from Schwarb et al., 2001). Other panels RCM simulation at 50 km (upper right), 25 km (lower left), and 12
 6 km (lower right) inter grid distance. (From Christensen et al., 2005).
 7
 8

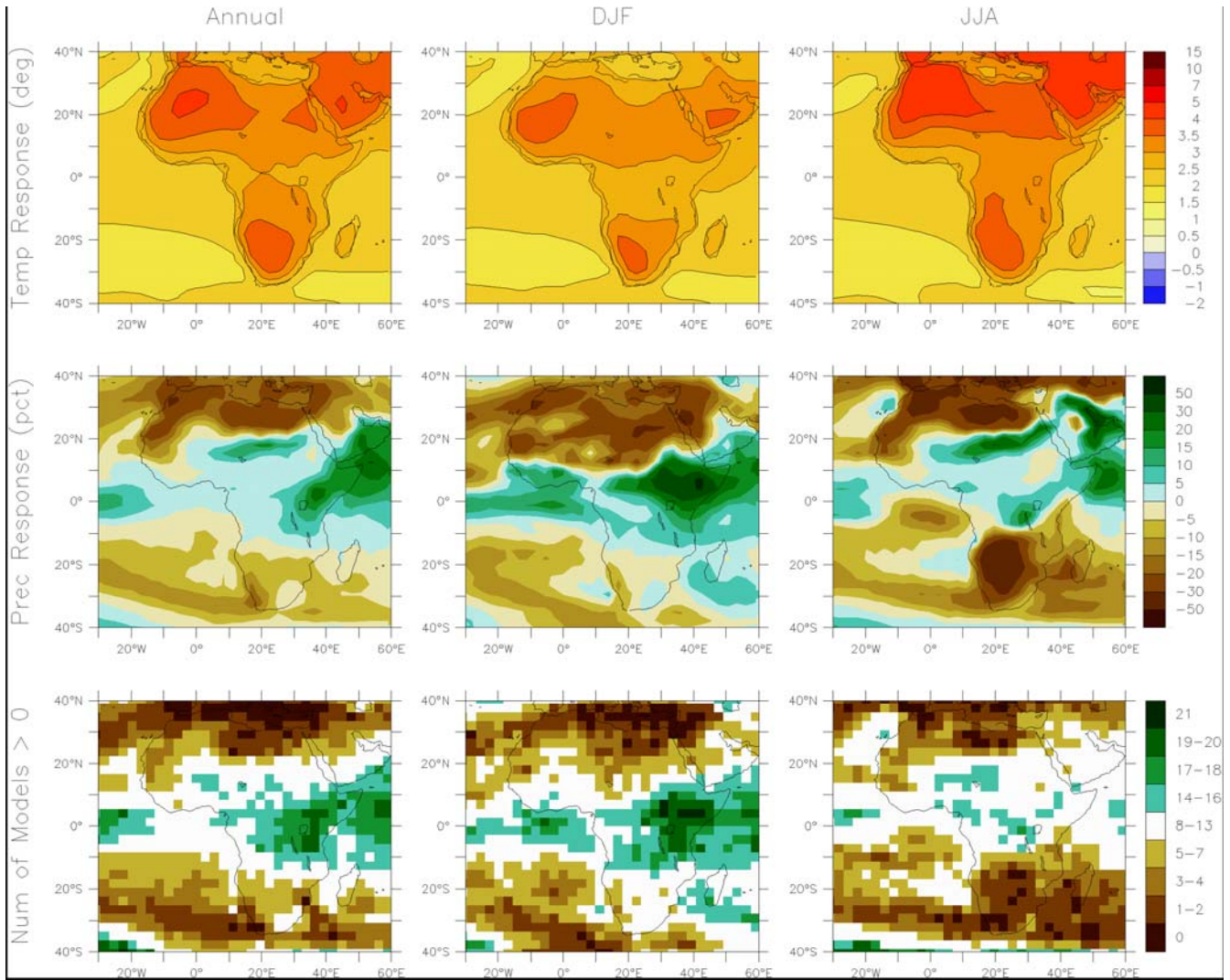
1



2
3
4
5
6
7

Figure 11.2.1. Quantiles of regional probability distributions derived by Greene et al. (2006) (top bar), Tebaldi et al. (2005) (bottom), and the empirical distribution of the AOGCM responses (middle bar) for temperature change in DJF under the A2 emissions scenario, at the end of the 21st century. Color bars indicate the 5–95% confidence interval. Lines through bars indicate the 25th, 50th, 75th, quantiles.

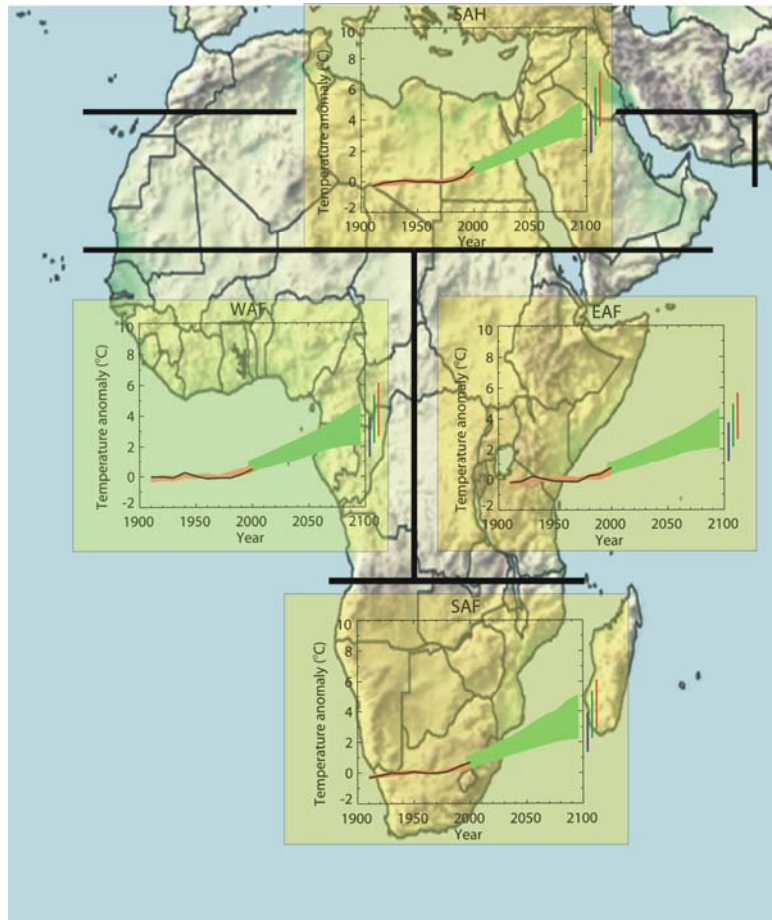
1
2



3
4
5
6
7
8
9
10

Figure 11.3.2.1. Consensus AR4 GCM A1B temperature and precipitation changes over Africa. Top row: Annual mean, December-January-February, and June-July-August temperature change between 1980–1999 in the 20C3M simulations and 2080–2099 in A1B, averaged over 21 models. Middle row: same for fractional change in precipitation. Bottom row: number of models out of 21 that project precipitation to increase.

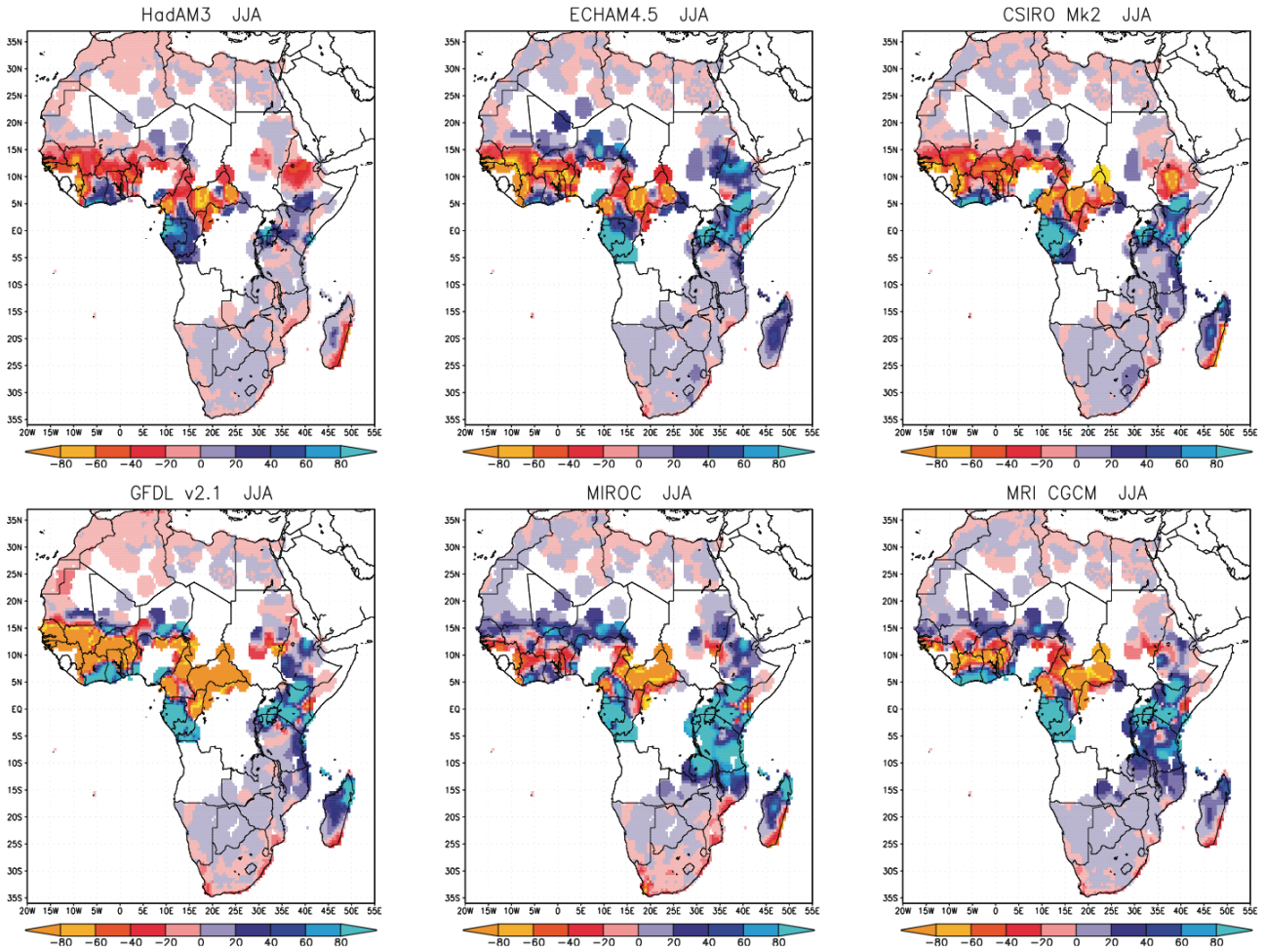
1
2



3
4
5
6
7
8
9

Figure 11.3.2.2. Warming for four African regions for: 1900–2000 as observed (black line) and as simulated (red envelope); and for 2001–2100 as simulated for the A1B emission scenario (green envelope). The set of AR4 AOGCM simulations used for both periods are only those with all forcings in the 20th century (eleven simulations).

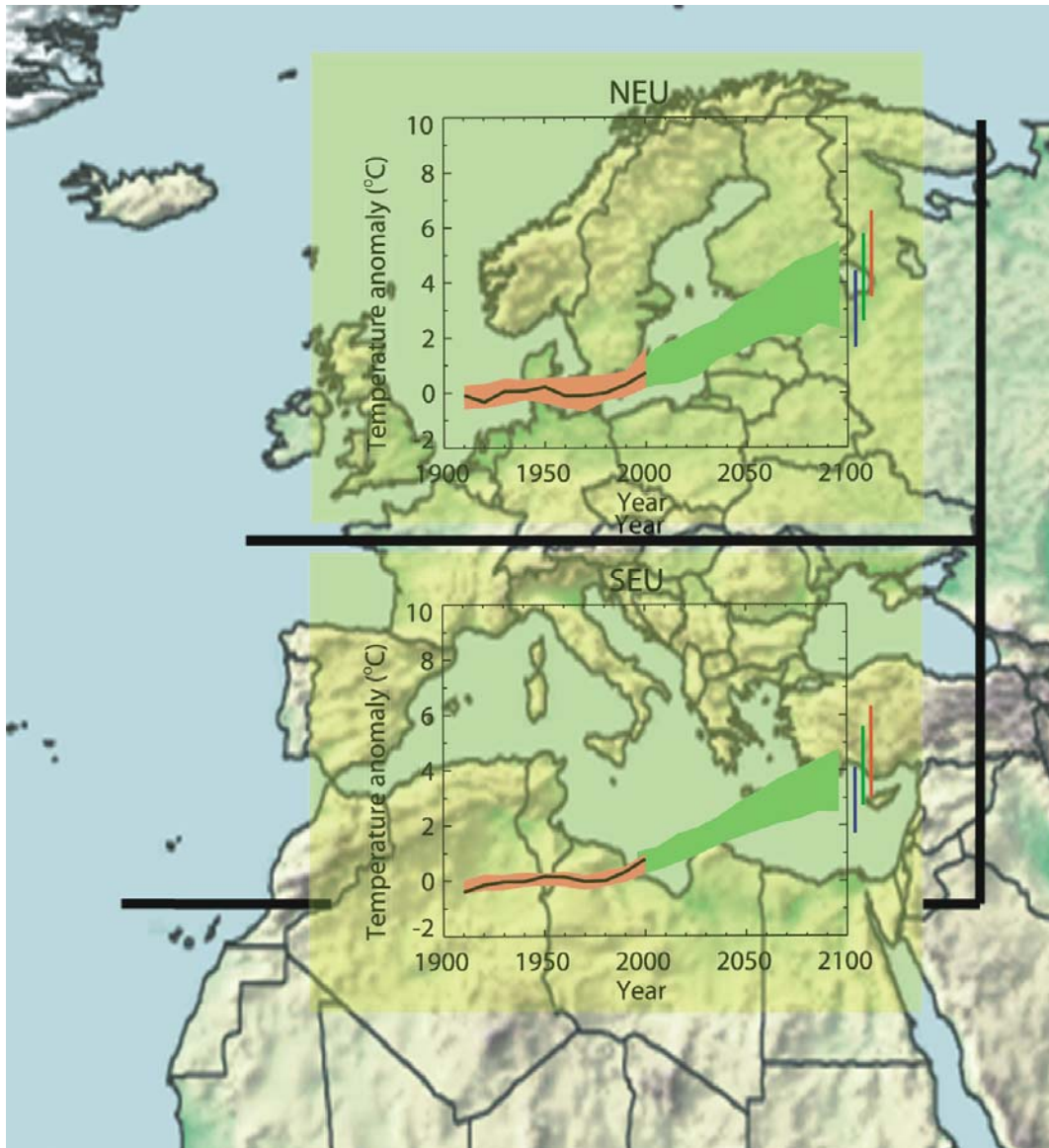
1
2



3
4
5
6
7
8
9
10

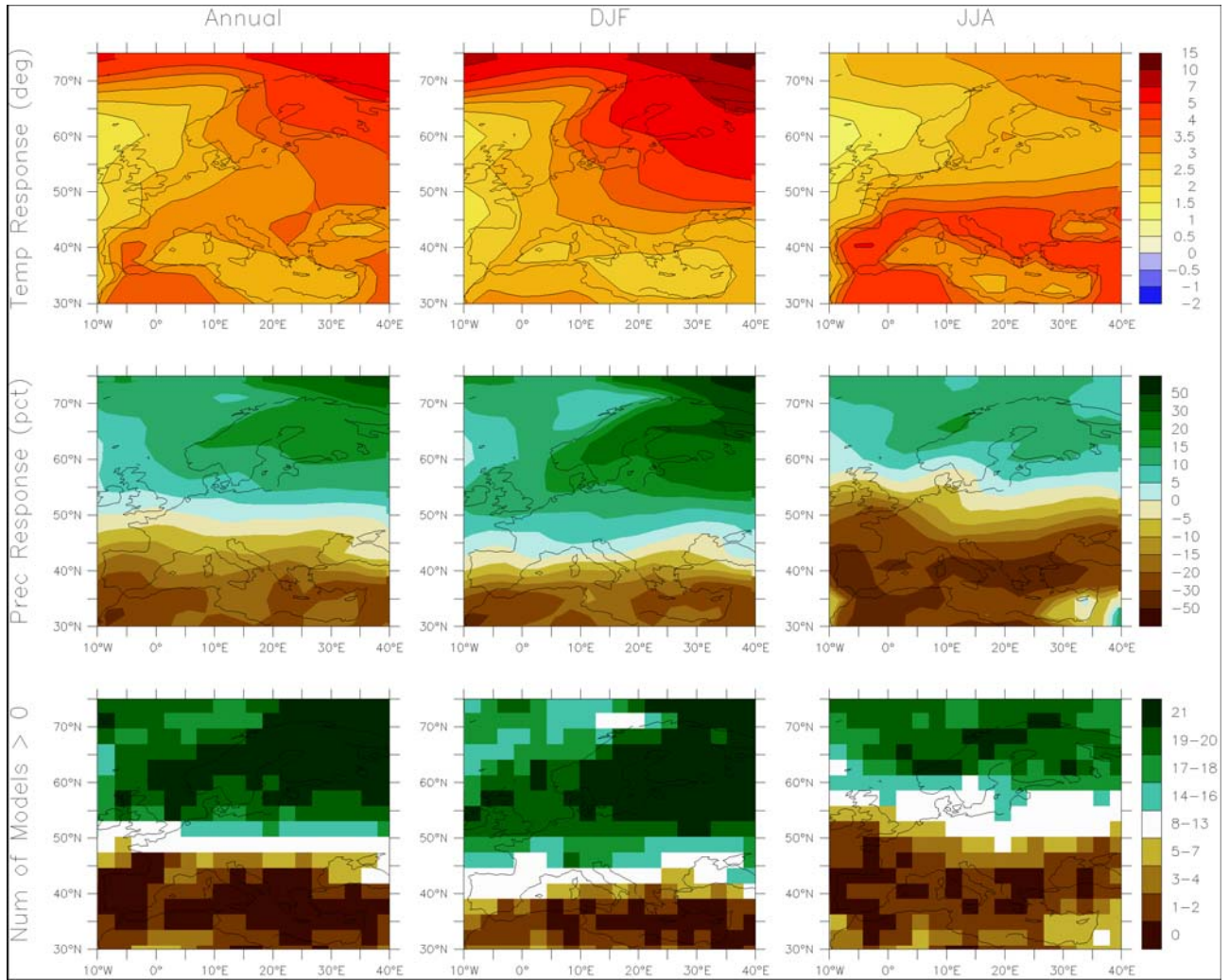
Figure 11.3.2.3. Anomaly of mean monthly precipitation (mm) daily data empirically downscaled from 6 GCMs (ECHAM4.5, HadAM3, CSIRO Mk2, GFDL 2.1, MRI, MIROC) to 858 station locations, and Cressman interpolated for plotting. GCMs are forced by the SRES A2 scenario. Anomalies are for the future period (2070–2099 for the first three models, and 2080–2099 for the latter three models) minus a control 30 year period.

1
2



3
4 **Figure 11.3.3.1.** Warming for northern and southern European regions for: 1900–2000 as observed (black
5 line) and as simulated (red envelope); and for 2001–2100 as simulated for the A1B emission scenario (green
6 envelope). The set of AR4 AOGCM simulations used for both periods are only those with all forcings in the
7 20th century (eleven simulations).
8

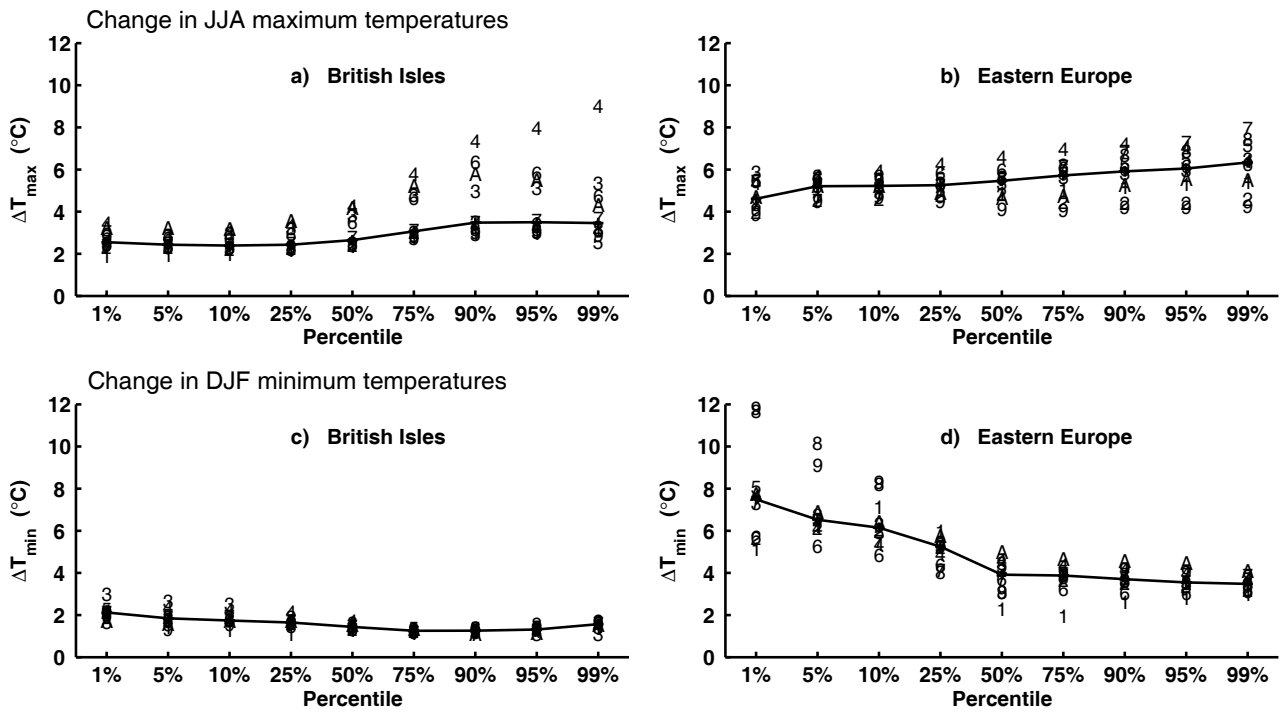
1
2



3
4
5
6
7
8
9
10

Figure 11.3.3.2. Consensus AR4 GCM A1B temperature and precipitation changes over Europe. Top row: Annual mean, December-January-February, and June-July-August temperature change between 1980–1999 in the 20C3M simulations and 2080–2099 in A1B, averaged over 21 models. Middle row: same for fractional change in precipitation. Bottom row: number of models out of 21 that project precipitation to increase

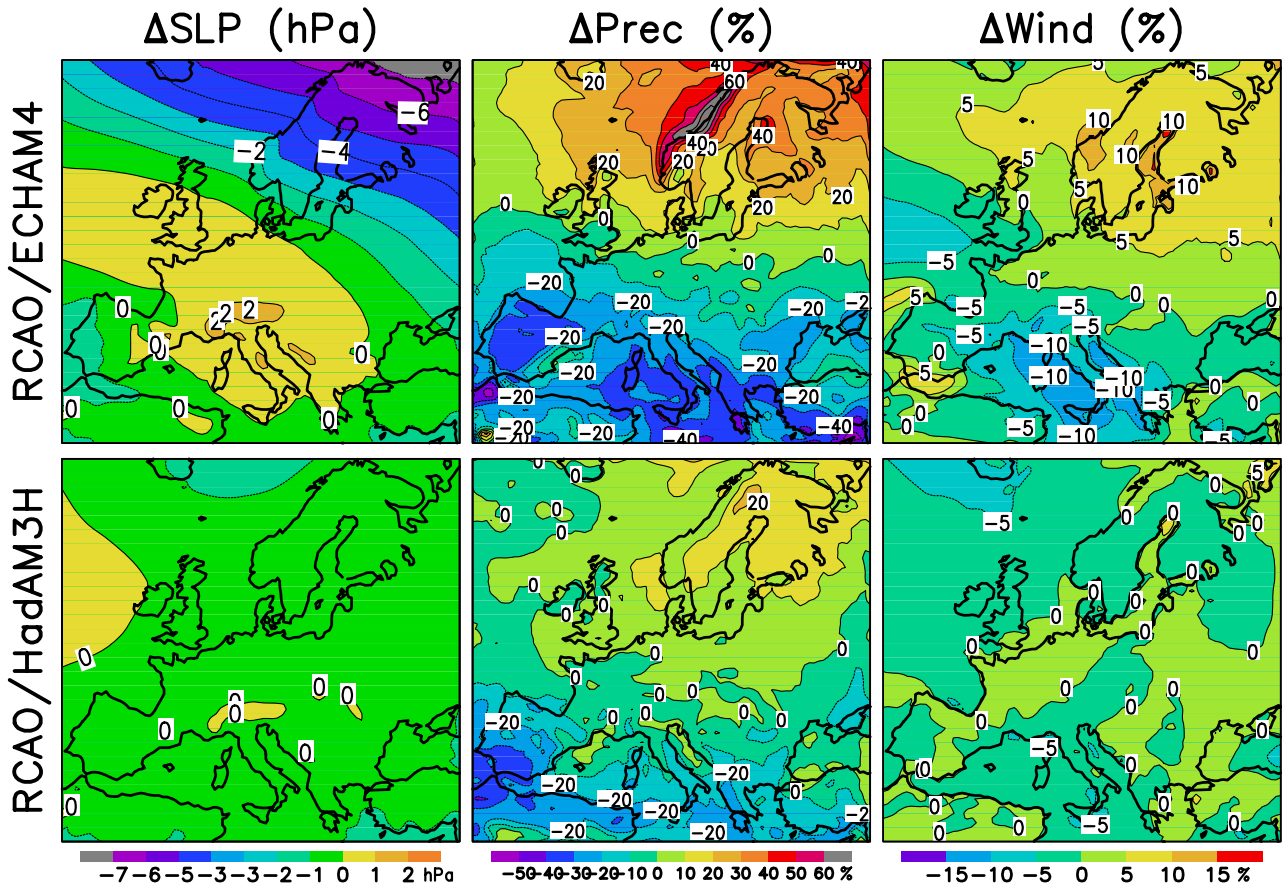
1
2



3
4
5
6
7
8
9
10
11

Figure 11.3.3.3. Changes in the distribution of JJA daily maximum temperatures (top) and DJF daily minimum temperatures (bottom) in the British Isles (left) and in eastern Europe in HadAM3H-driven PRUDENCE simulations (from 1961–1990 to 2071–2100 under the SRES A2 scenario). The horizontal axis gives the percentile of the distribution; for example, 95% of the daily minimum or maximum temperatures are below the 95th percentile. The vertical axis gives the changes in each percentile (in °C) separately for ten RCMs (1–9 and A). The lines show the median of the RCM projections (based on Kjellström et al., 2006).

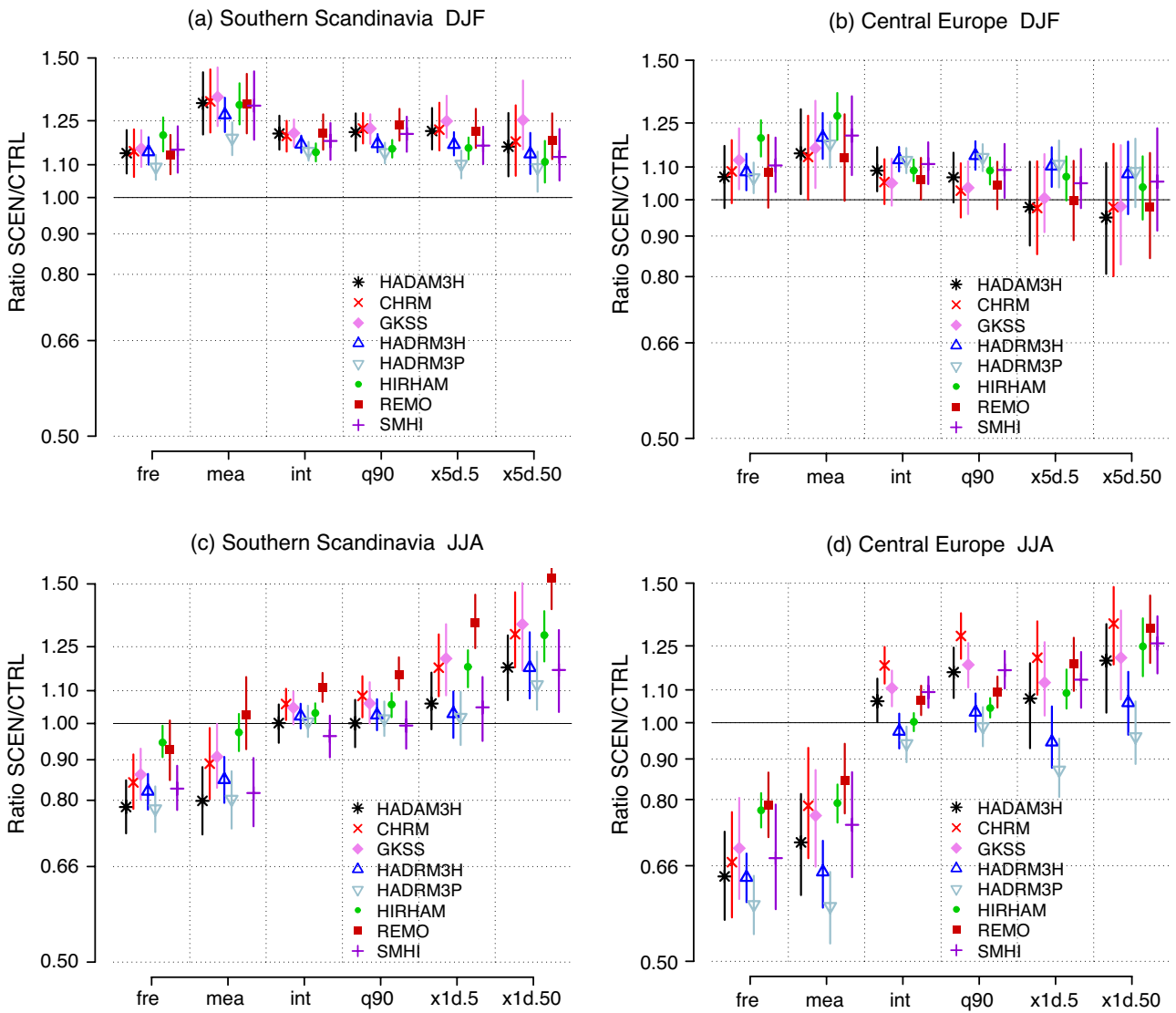
1
2



3
4
5
6
7
8
9
10

Figure 11.3.3.4. Simulated changes in annual mean sea level pressure (Δ SLP), precipitation (Δ Prec) and mean 10 m level wind speed (Δ Wind) from the years 1961–1990 to the years 2071–2100. The results are based on the SRES A2 scenario and were produced by the same RCM (RCAO) using boundary data from two global models: ECHAM4/OPYC3 (top) and HadAM3H (bottom) (redrawn from Rummukainen et al., 2004).

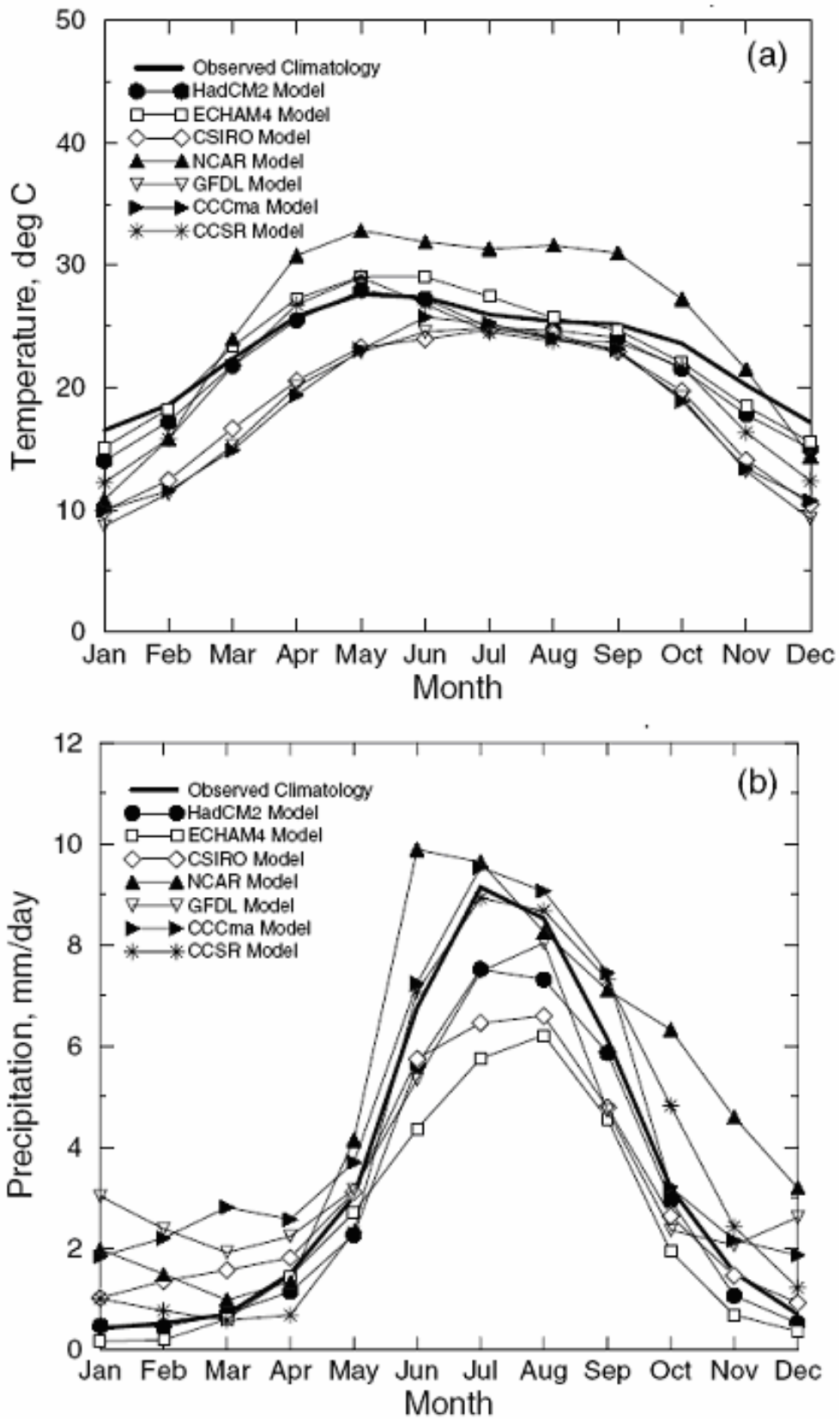
1
2



3
4
5
6
7
8
9
10
11
12

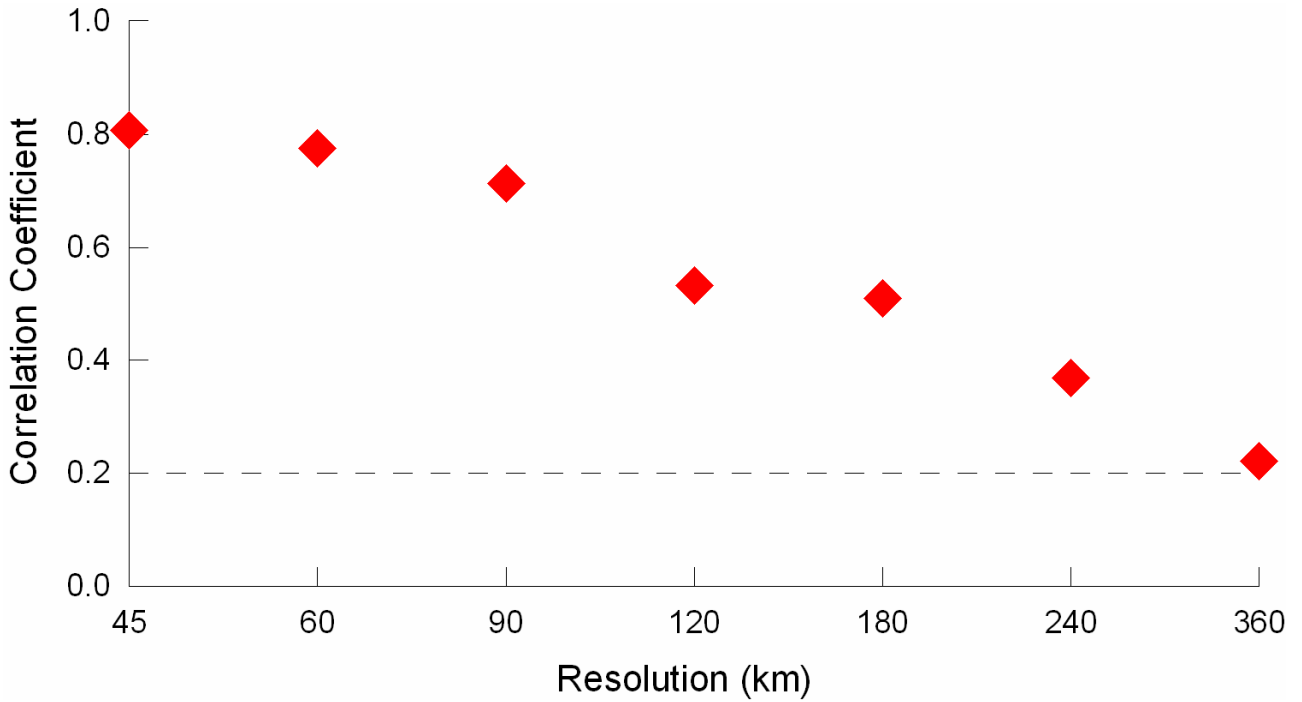
Figure 11.3.3.5. Changes (ratio 2071–2100/1961–1990 for the A2 scenario) in domain-mean precipitation diagnostics in the PRUDENCE simulations in southern Scandinavia (5–20°E, 55–62°N) and central Europe (5–15°E, 48–54°N) in winter (top) and in summer (bottom). *fre* = wet-day frequency; *mea* = mean seasonal precipitation; *int* = mean wet-day precipitation; *q90* = 90th percentile of wet-day precipitation; *x1d.5* and *x1d.50* = 5- and 50-year return values of one-day precipitation; *x5d.5* and *x5d.50* = 5- and 50-year return values of five-day precipitation. For each of the eight models, the vertical bar gives the 95% confidence interval associated with sampling uncertainty (redrawn from Frei et al., 2006).

1
2



3
4 **Figure 11.3.4.1.** Validation of simulated and observed area-averaged annual cycle of (a) surface air
5 temperature and (b) precipitation over South Asia. (After Lal and Harasawa, 2000).
6

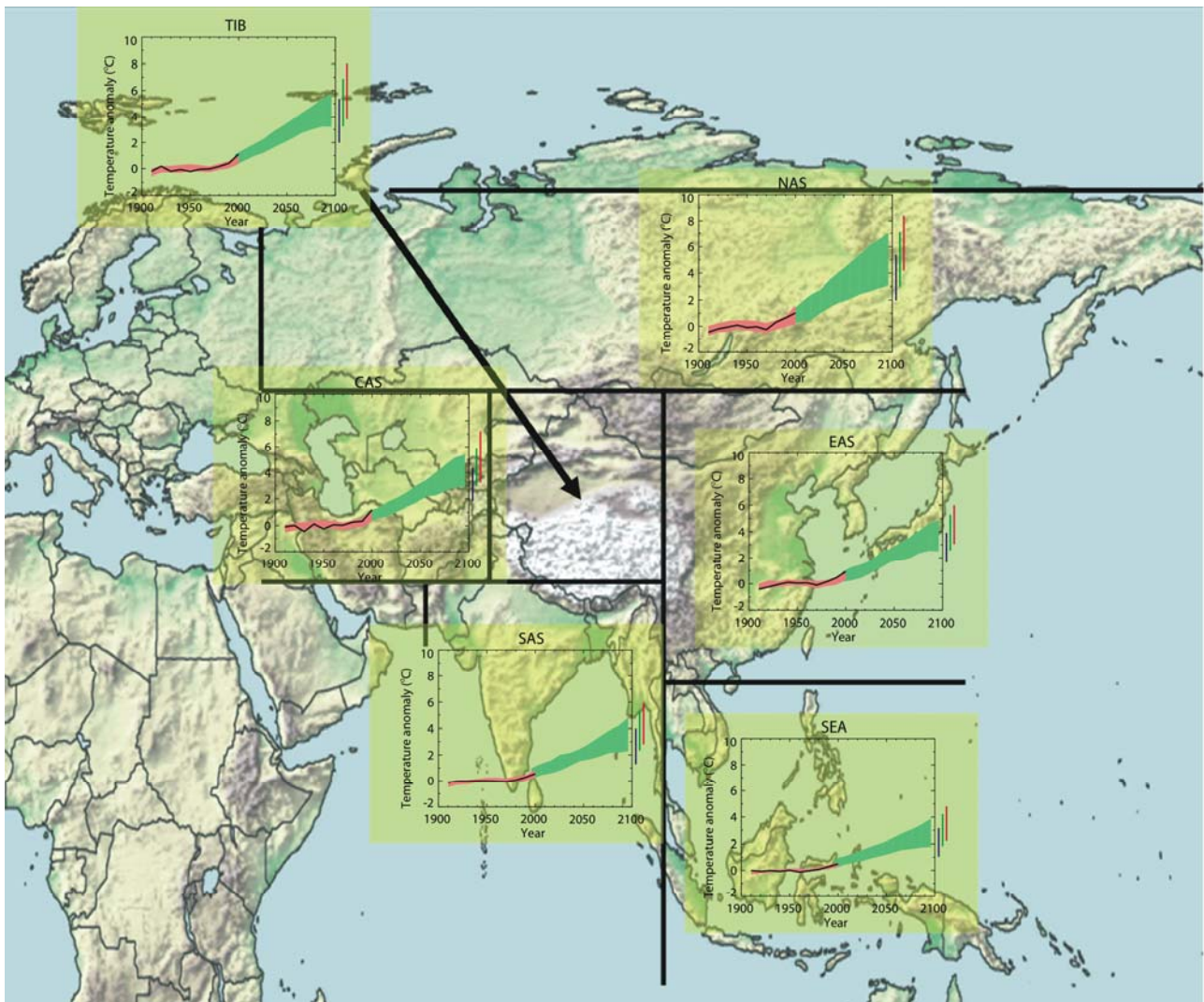
1
2



3
4
5
6
7
8

Figure 11.3.4.2. Spatial correlation coefficient between simulated and observed annual mean precipitation by different horizontal resolutions of a RCM (dashed line is 0.99 significant level). Adapted from Gao et al. (2006).

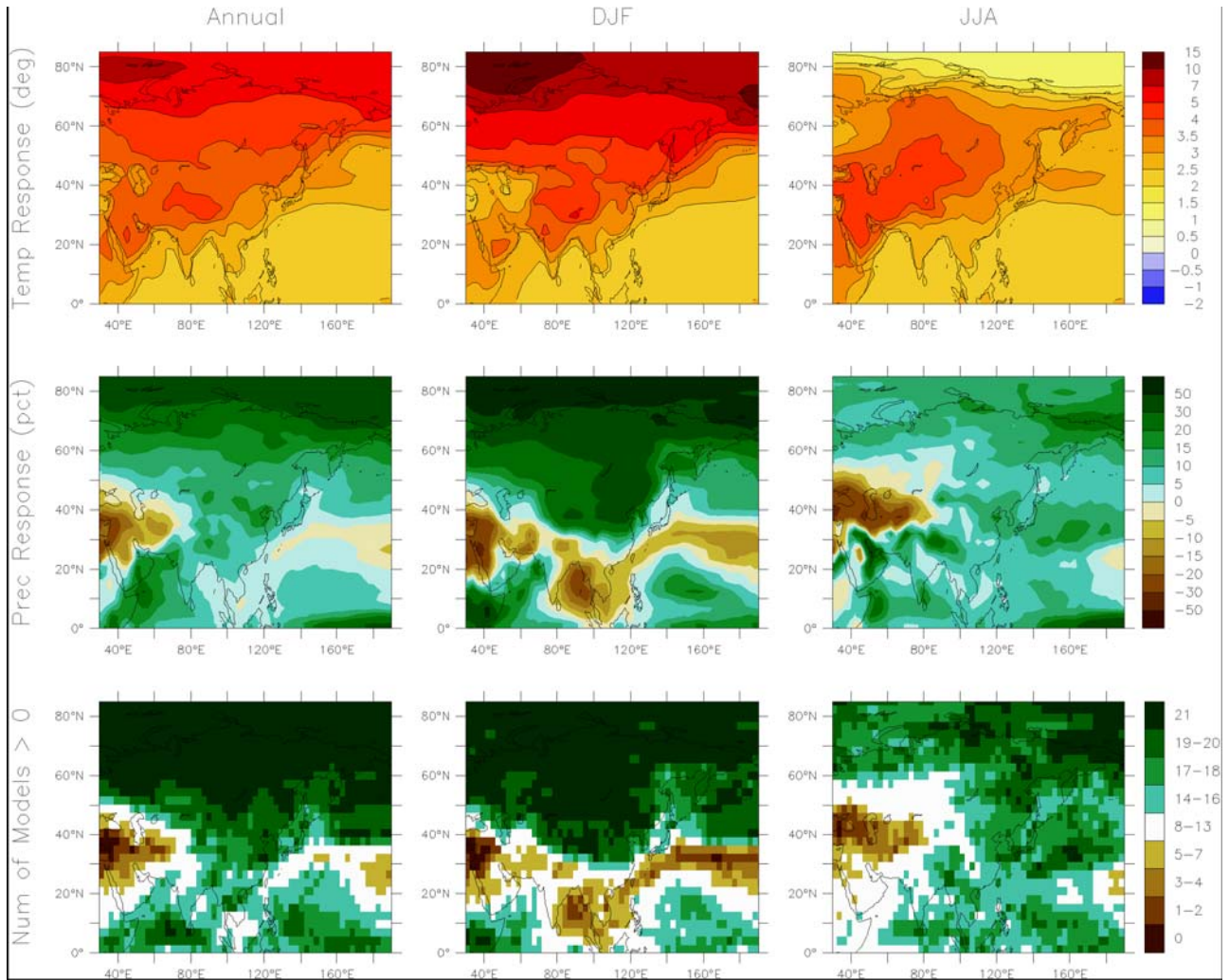
1
2
3



4
5
6
7
8
9
10

Figure 11.3.4.3. Warming for six Asian regions for: 1900–2000 as observed (black line) and as simulated (red envelope); and for 2001–2100 as simulated for the A1B emission scenario (green envelope). The set of AR4 AOGCM simulations used for both periods are only those with all forcings in the 20th century (eleven simulations).

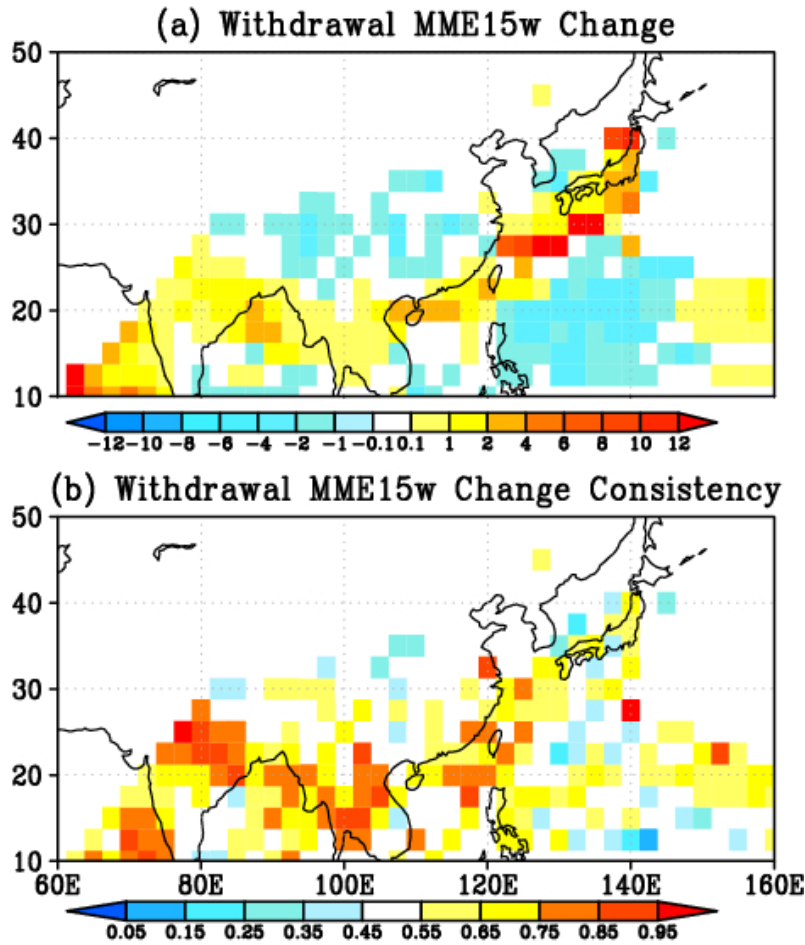
1
2



3
4
5
6
7
8
9
10

Figure 11.3.4.4. Consensus AR4 GCM A1B temperature and precipitation changes over Asia. Top row: Annual mean, December-January-February, and June-July-August temperature change between 1980–1999 in the 20C3M simulations and 2080–2099 in A1B, averaged over 21 models. Middle row: same for fractional change in precipitation. Bottom row: number of models out of 21 that project precipitation to increase.

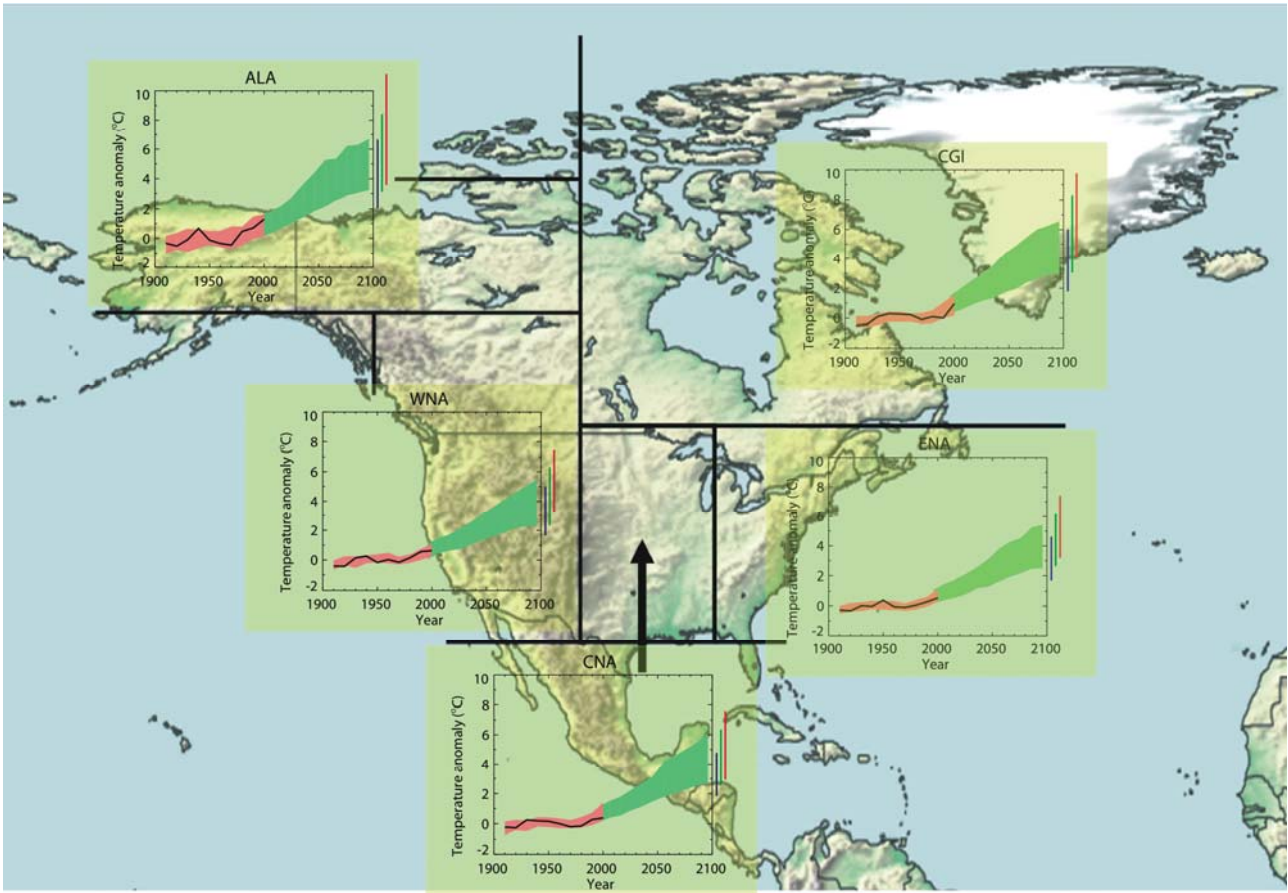
1
2



3
4
5
6
7
8
9

Figure 11.3.4.5. (a) Changes in withdrawal dates (pentad) of the Asian summer rainy season based on the 15 AOGCM ensemble climatological pentad mean precipitation between the 2081–2100 of the SRES A1B experiments and the present day (1981–2000) of the 20C3M experiments. (b) Fraction of model numbers with positive difference of onset dates from the present to the future. (Kitoh and Uchiyama 2006)

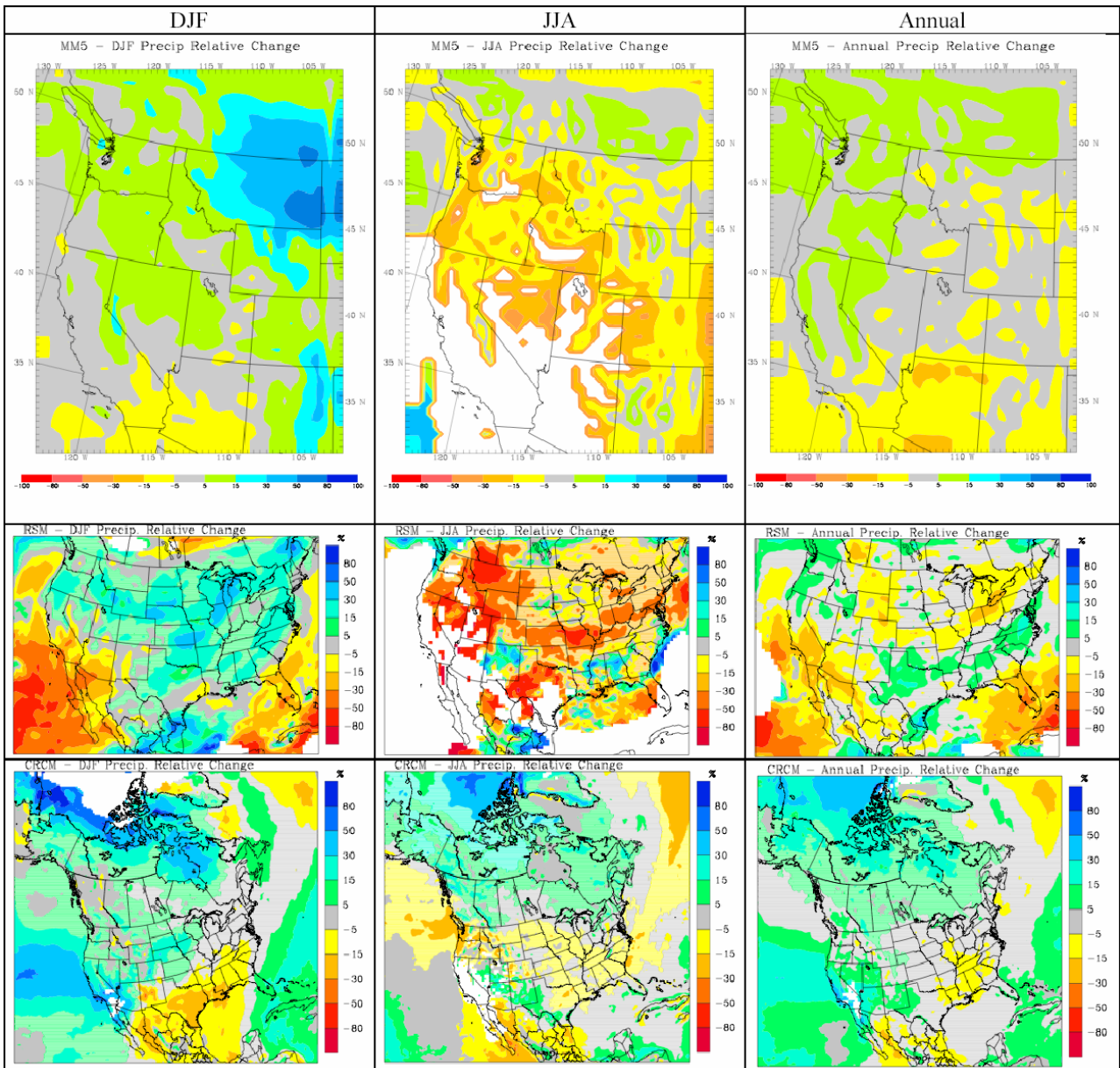
1
2



3
4
5
6
7
8

Figure 11.3.5.1. Warming for five North American regions for: 1900–2000 as observed (black line) and as simulated (red envelope); and for 2001–2100 as simulated for the A1B emission scenario (green envelope). The set of AR4 AOGCM simulations used for both periods are only those with all forcings in the 20th century (eleven simulations).

1
2



3
4
5

[CONTINUED ON NEXT PAGE]